Supporting Information for

Dual carbon isotope-based source apportionment and light absorption properties of water soluble organic carbon in $PM_{2.5}$ over China

Yangzhi Mo[1], Jun Li[1*], Zhineng Cheng[1], Guangcai Zhong[1], Sanyuan Zhu[1], Chongguo Tian[2], Yingjun Chen[3], Gan Zhang[1*]

[1] State Key Laboratory of Organic Geochemistry and Guangdong Key Laboratory of Environmental Protection and Resources Utilization, Guangzhou Institute of Geochemistry, Chinese Academy of Sciences, Guangzhou 510640, China

[2] Key Laboratory of Coastal Zone Environmental Processes and Ecological Remediation, Yantai Institute of Coastal Zone Research, Chinese Academy of Science, Yantai, 264003, China

[3]Shanghai Key Laboratory of Atmospheric Particle Pollution and Prevention, Department of Environmental Science and Engineering, Fudan University, Shanghai 200433, China

*Corresponding author: Dr. Jun Li

Tel: +86-20-85291508; Fax: +86-20-85290706; E-mail: junli@gig.ac.cn

Corresponding author: Dr. Gan Zhang

Tel: +86-20-85290805; Fax: +86-20-85290706; E-mail: zhanggan@gig.ac.cn

Numbers of Pages: 15
Numbers of Tables: 9
Numbers of Figures: 3

Stable carbon and radiocarbon analyses

For stable carbon analysis, WSOC was extracted as described above. And then, 30–50 μgC of WSOC was re-dissolved in ultrapure water and transferred into a tin capsule (Elementar, Germany). After evaporation in an oven at 60°C, the stable isotopic composition ($\delta^{13}C$) was then measured using an elemental analyzer (EA, Model Vario Micro, Elementar, Germany) interfaced to a Finnigan MAT-252 mass spectrometer (Thermo Electron Corporation, USA). The $\delta^{13}C$ results were presented as relative to that of a standard, Vienna Pee Dee Belemnite. Samples were analyzed at least three times, and the analytical error in the carbon isotope ratios was within 0.3‰.

In a similar procedure to stable carbon analysis, more than 150 μg C of WSOC was packed in the tin capsules and then combusted to CO_2 by the elemental analyzer. Further, the CO_2 was reduced into graphite targets by graphitization line at Guangzhou Institute of Geochemistry of the Chinese Academy of Sciences (CAS) via the hydrogen and zinc reduction method and then the ^{14}C content of graphite samples was measured at the National Electrostatics Corporation compact accelerator mass spectrometry facility (AMS) at Guangzhou Institute of Geochemistry, CAS (Guangzhou, China)(Zhu et al., 2015). AMS calibration was performed using standards (Oxalic Acid Standards I and II) and blanks. The $\delta^{13}C$ value was obtained during AMS measurements and applied to correct the ^{14}C measurements for isotopic fractionation. The ^{14}C results are presented as fraction of modern (f_m) denoting the $^{14}C/^{12}C$ content of the sample related to that of the reference year 1950.(Levin et al., 2010; Mohn et al., 2008) To eliminate the effects of thermonuclear weapon tests in the 1950s and 1960s, the f_m was converted into the fraction of non-fossil carbon (f_{nf}) with a correction factor of 1.08 ± 0.05 based on the long-term time series of $^{14}CO_2$ at the background station, so the f_{nf} is calculated by $f_{nf} = f_m/1.08$. The f_{nf} can range from 0 (pure fossil carbon) to 1 (pure modern carbon) and directly reflects the relative fossil and non-fossil contribution to carbon. The uncertainties of f_{nf} was estimated from an error propagation, and included uncertainties in the concentration, variability of the reference $f_{m,nf}$, and measurement uncertainty of f_m. The average uncertainties of f_{nf} for WSOC was 2.79 ± 0.43 %.

Table S1. Information of sampling sites

Regions	Provrince (Urbanization rate %)[a]	City	Latitude (°N)	Longitude (°E)	Season	Samples Number
Northern China	Beijing (86.3)	Beijing (BJ)	39.93	116.34	Spring	29
					Summer	25
					Fall	22
					Winter	19
	Henan (39.3)	Xinxiang (XX)	35.33	113.91	Spring	29
					Summer	29
					Fall	21
					Winter	25
	Shanxi (52.6)	Taiyuan (TY)	37.54	112.33	Spring	31
					Summer	30
					Fall	26
					Winter	31
	Gansu (40.1)	Lanzhou (LZ)	36.05	103.86	Spring	28
					Summer	30
					Fall	27
					Winter	28
Southern China	Shanghai (88.0)	Shanghai (SH)	31.29	121.5	Spring	31
					Summer	23
					Fall	25
					Winter	29
	Jiangsu (62.9)	Nanjing (NJ)	32.06	118.8	Spring	22
					Summer	25
					Fall	25
					Winter	22
	Sichuan (44.9)	Chengdu (CD)	30.64	104.08	Spring	28
					Summer	29
					Fall	26
					Winter	30
	Guizhou (37.8)	Guiyang (GY)	26.57	106.73	Fall	22
					Winter	32
	Hubei (54.5)	Wuhan (WH)	30.53	114.37	Spring	23
					Summer	27
					Fall	22
					Winter	25
	Guangdong (67.8)	Guangzhou (GZ)	23.15	113.36	Spring	25
					Summer	27
					Fall	25
					Winter	22

[a] The urbanization rate of different provinces in 2013 was obtained from National Bureau of Statistics.

Table S2. The $\delta^{13}C$ values for source sampling reported in previous studies.

Sources	$\delta^{13}C$ values (‰)	$\delta^{13}C$ (‰) used in the Bayesian mixing model calculations (mean ± standard deviation).	References
Liquid fossil fuel	-29.0 to -23.6	-25.6 ± 1.8	(Agnihotri et al., 2011; Ancelet et al., 2011; Chen et al., 2012; Dai et al., 2015; Guo et al., 2016; Huang et al., 2006; Kawashima and Haneishi, 2012; López-Veneroni, 2009; Widory, 2006)
Coal combustion	-24.15 to -21.7	-23.4 ± 1.3	(Agnihotri et al., 2011; Chen et al., 2012; Guo et al., 2016; Kawashima and Haneishi, 2012; Widory, 2006)
C3 plants	-34.7 to -24.6	-28.2 ± 2.3	(Agnihotri et al., 2011; Ancelet et al., 2013; Chen et al., 2012; Das et al., 2010; Guo et al., 2016; Kawashima and Haneishi, 2012; Liu et al., 2014; Wang et al., 2013)
C4 plants	-19.3 to -12.3	-14.6 ± 2.6	(Chen et al., 2012; Das et al., 2010; Guo et al., 2016; Kawashima and Haneishi, 2012; Liu et al., 2014)

Table S3. Concentrations (ugC/m^3) of WSOC in $PM_{2.5}$ from 10 Chinese cities.

	Spring	Summer	Fall	Winter
Beijing	8.90	5.54	9.46	11.9
Xinxiang	7.00	2.68	10.1	15.6
Taiyuan	8.84	5.39	8.01	9.59
Lanzhou	4.70	3.85	7.87	12.95
Shanghai	3.82	2.89	4.06	9.05
Nanjing	4.25	3.13	5.95	6.57
Chengdu	5.53	4.30	6.23	10.4
Guiyang[a]	N.D	N.D	4.35	10.3
Wuhan	3.89	4.25	6.39	7.80
Guangzhou	4.02	3.92	7.46	10.3
AVG[a]	5.66	3.99	6.72	10.3
SD[b]	2.08	1.01	1.90	2.70

[a] Guiyang just contains fall and winter samples.
[b] AVG: Arithmetic average.
[c] SD: Standard deviation.

Table S4. The average temperature and precipitation at ten cities during the sampling campaign.

City	Temperature (℃)				Precipitation (mm)			
	Spring	Summer	Fall	Winter	Spring	Summer	Fall	Winter
BJ	17.0	26.3	10.3	0.3	20.8	52.3	12.6	3.0
XX	16.9	25.9	13.7	4.3	56.4	67.7	29.8	0.2
TY	14.5	23.0	10.6	0.5	55.6	131.1	37.6	18.8
LZ	21.7	28.5	19.3	0.1	135.0	244.6	60.4	84.9
SH	16.0	26.6	16.8	6.7	139.4	271.4	156.1	35.8
NJ	16.5	25.9	15.8	5.8	97.5	161.5	21.5	15.6
CD	20.3	28.2	17.7	9.3	93.6	239.9	74.0	11.1
GY	17.2	23.5	13.8	6.1	37.5	167.2	52.8	24.7
WH	17.7	26.7	15.8	6.1	107.3	145.5	30.1	19.5
GZ	23.2	29.0	22.0	13.7	192.7	513.3	23.6	53.0
AVG[a]	18.1	26.4	15.6	6.3	93.6	199.5	49.8	26.6
SD[b]	2.7	2.0	3.7	4.2	52.8	131.8	41.9	25.6

[a] AVG: Arithmetic average.
[b] SD: Standard deviation.

Table S5. MAE_{365} and AAE of WSOC in $PM_{2.5}$ from 10 Chinese cities.

	$MAE_{365}(m^2/gC)$				AAE			
	Spring	Summer	Fall	Winter	Spring	Summer	Fall	Winter
Beijing	0.86	0.67	1.32	1.71	5.7	5.2	6.8	5.6
Xinxiang	0.99	0.91	1.4	1.65	5.1	3.8	4. 8	5.2
Taiyuan	0.95	0.96	1.64	1.76	5.7	5.1	5.2	6.3
Lanzhou	1.02	0.76	1.86	1.6	5.7	5.2	4.2	4.7
Shanghai	0.74	0.55	0.83	1.34	5.4	5.7	5.6	5.3
Nanjing	1.09	0.78	1.37	1.67	4.9	5.3	4.9	5.1
Chengdu	0.79	0.72	1.27	1.21	5.3	5.7	5.7	5.7
Guiyang[a]	N.D	N.D	1.16	1.53	N.D	N.D	4.4	5
Wuhan	0.85	0.73	1.34	1.65	5.4	5.6	5.1	4.8
Guangzhou	0.78	0.68	0.88	1.03	6	5.9	5.8	5.8
AVG[b]	0.95	0.75	1.25	1.49	5.5	5.3	5.1	5.3
SD[c]	0.17	0.12	0.37	0.24	0.3	0.6	0.6	0.5

[a] Guiyang just contains fall and winter samples.
[b] AVG: Arithmetic average.
[c] SD: Standard deviation.

Table S6. Correlation coefficients (r) of Abs_{365} with WSOC and water soluble ions.

	$Abs_{365, WSOC}$	
	Warm seasons	Cold seasons
WSOC	0.92^{*}	0.92^{*}
K^+	$0.54^{\#}$	0.74^{*}
NO_3^-	0.85^{*}	$0.52^{\#}$
SO_4^{2-}	0.64^{*}	$0.56^{\#}$
NH_4^+	0.73^{*}	$0.48^{\#}$

* $p < 0.01$
$^{\#}$ $p < 0.05$

Table S7. The annual average $\delta^{13}C$ and non-fossil contribution of WSOC.

	$\delta^{13}C$ (‰)		Non-fossil contribution	
	WSOC	SD	WSOC	SD
Beijing	-23.7	0.7	0.56	0.06
Xinxiang	-23.4	1.1	0.58	0.03
Taiyuan	-23.4	0.9	0.47	0.06
Lanzhou	-24.2	0.7	0.61	0.05
Shanghai	-24	0.9	0.58	0.11
Nanjing	-24.6	0.6	0.56	0.06
Chengdu	-24.9	0.9	0.69	0.05
Guiyang[a]	-22.9	0.8	0.78	0.04
Wuhan	-24.3	0.8	0.67	0.04
Guangzhou	-24.7	0.6	0.59	0.1

[a] Guiyang just contains fall and winter samples.

Table S8. The annual average concentration of water soluble ions.

	Cl^-	SD	NO_3^-	SD	SO_4^{2-}	SD	K^+	SD	Na^+	SD	NH_4^+	SD
Beijing	2.58	2.17	14.0	5.89	11.6	1.96	1.05	0.51	0.59	0.32	7.84	2.49
Xinxiang	4.06	3.65	17.4	10.0	20.7	10.3	1.70	1.15	0.64	0.44	9.56	5.31
Taiyuan	6.43	6.06	14.5	5.96	27.2	4.21	1.49	0.70	0.96	0.54	9.87	1.96
Lanzhou	3.71	2.95	9.79	6.29	13.6	4.85	1.43	0.94	1.23	0.59	3.63	2.92
Shanghai	1.38	1.51	9.59	6.71	9.28	3.85	0.62	0.44	0.49	0.14	5.53	2.92
Nanjing	1.10	1.01	10.9	5.25	10.4	3.84	0.85	0.49	0.24	0.08	6.84	2.74
Chengdu	1.29	0.87	9.27	4.42	11.2	3.51	0.76	0.49	0.28	0.07	7.05	2.82
Guiyang[a]	0.41	0.29	4.22	3.71	15.5	5.97	0.90	0.44	0.17	0.09	6.32	2.65
Wuhan	0.74	0.80	8.86	5.23	11.7	2.55	0.92	0.45	0.20	0.04	6.52	2.13
Guangzhou	0.60	0.47	6.61	5.80	15.3	8.13	1.30	0.62	0.58	0.12	7.53	4.66

[a] Guiyang just contains fall and winter samples.

Table S9. Multiple linear regression between Abs_{365} and concentration of fossil and non-fossil sources WSOC in China.

Model: R^2 = 0.891 Adjusted R^2 = 0.884	Unstandardized coefficients		*t*-STAT	*p*-Value
	B	Standard error		
Constant	-4.127	0.801	-5.154	0.000
Fossil sources concentration	2.148	0.302	7.109	0.000
Non-fossil sources concentration	1.641	0.206	7.963	0.000

Figure S1. Cluster analysis of 5-day backward trajectories and the spatial distributions of active fire spots over China during the sampling campaign. Cluster analysis is performed by HYSPLIT. Red dots represent fire count data obtained from Fire Information for Resource Management System (FIRMS) acquired by the Moderate Resolution Imaging Spectroradiometer (MODIS) satellite for the sampling days. The basemap was created by ArcGIS software (Source: ESRI Inc. CA).

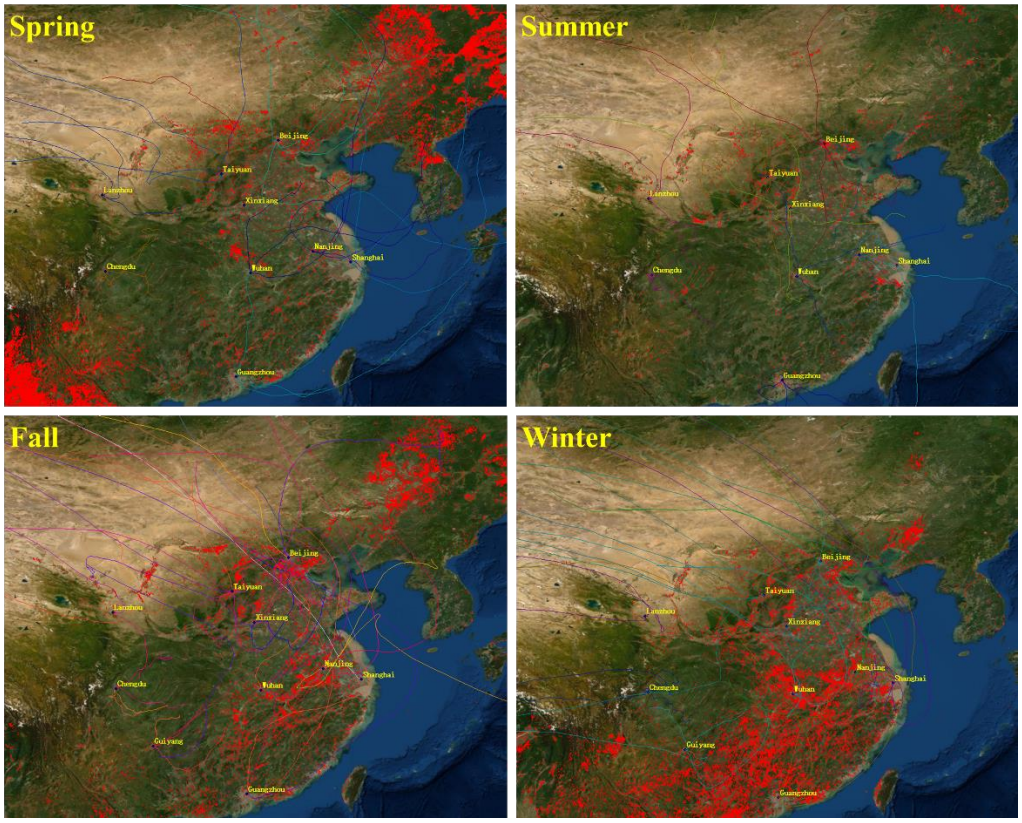

Figure S2. The median contributions and concentrations of liquid fossil fuel, coal combustion, C3 plants and C4 plants of WSOC by Bayesian source appointment model. The red line is the median of contribution and the orange region refers to the interquartile range (25^{th} to 75^{th}).

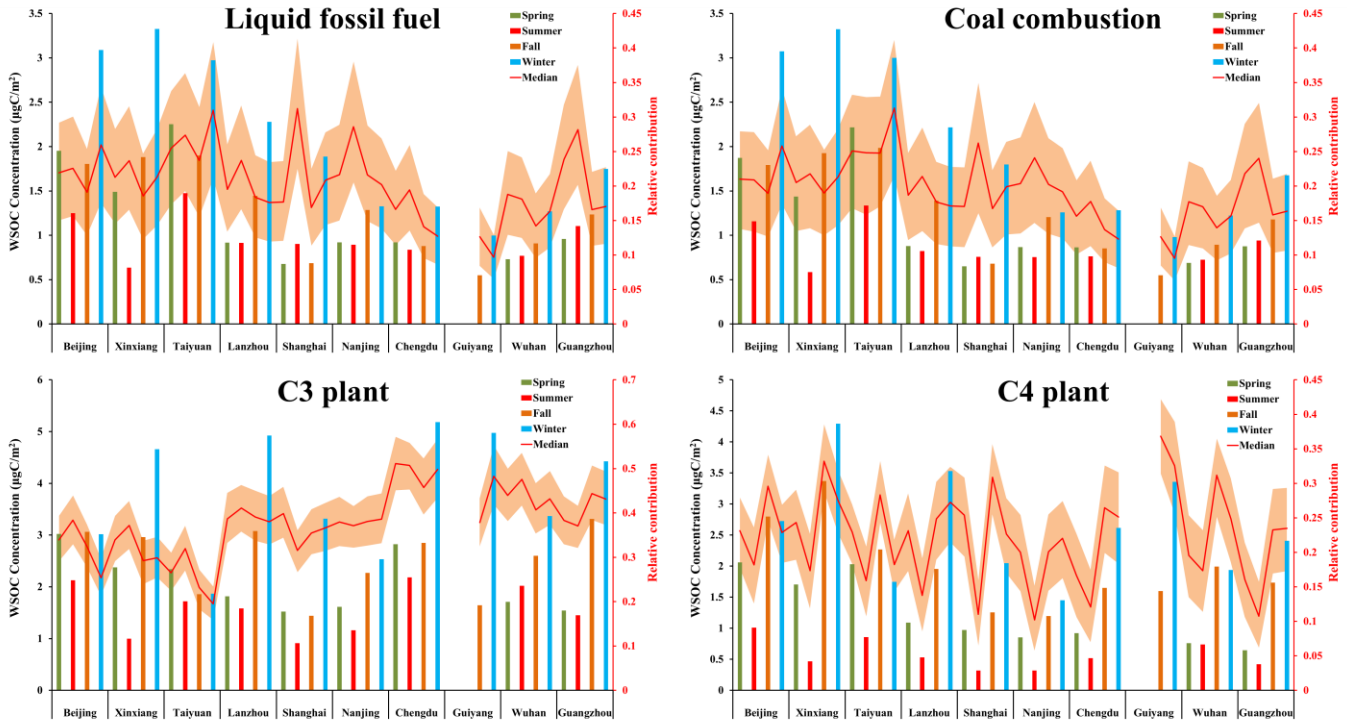

Figure S3. The distribution of main corn area in China. (https://www.fas.usda.gov/data/summer-drought-limits-upside-potential-china-corn-yields).

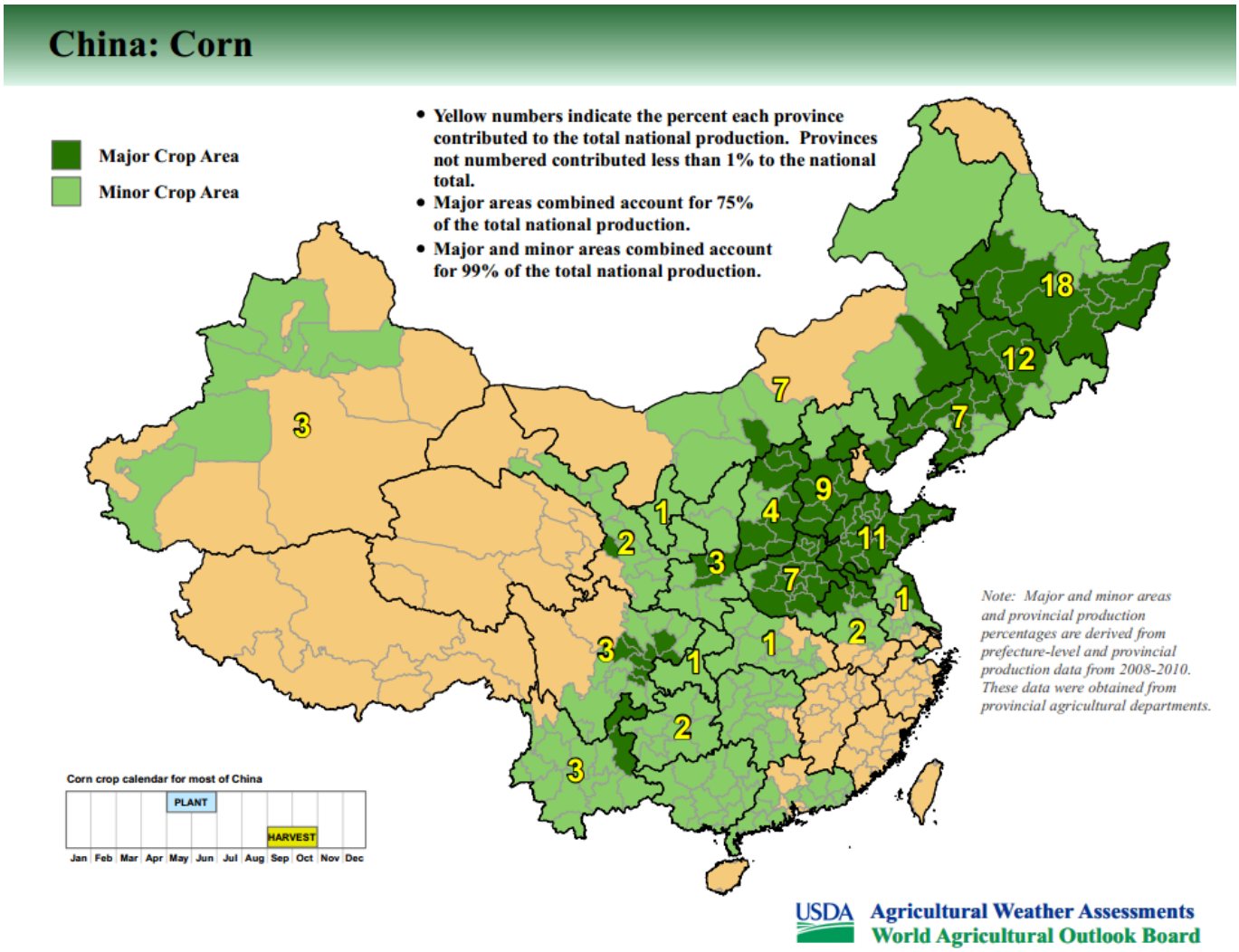

177
178

References:

Agnihotri, R., Mandal, T., Karapurkar, S., Naja, M., Gadi, R., Ahammmed, Y.N., Kumar, A., Saud, T., Saxena, M., 2011. Stable carbon and nitrogen isotopic composition of bulk aerosols over India and northern Indian Ocean. Atmospheric Environment 45, 2828-2835.

Ancelet, T., Davy, P.K., Trompetter, W.J., Markwitz, A., Weatherburn, D.C., 2011. Carbonaceous aerosols in an urban tunnel. Atmospheric Environment 45, 4463-4469.

Ancelet, T., Davy, P.K., Trompetter, W.J., Markwitz, A., Weatherburn, D.C., 2013. Carbonaceous aerosols in a wood burning community in rural New Zealand. Atmospheric Pollution Research 4, 245-249.

Chen, Y., Cai, W., Huang, G., Li, J., Zhang, G.J.H.j.k.x.H.k., 2012. Stable carbon isotope of black carbon from typical emission sources in China. 33, 673-678.

Dai, S., Bi, X., Chan, L., He, J., Wang, B., Wang, X., Peng, P., Sheng, G., Fu, J., 2015. Chemical and stable carbon isotopic composition of PM 2.5 from on-road vehicle emissions in the PRD region and implications for vehicle emission control policy. Atmospheric Chemistry and Physics 15, 3097-3108.

Das, O., Wang, Y., Hsieh, Y.-P.J.O.G., 2010. Chemical and carbon isotopic characteristics of ash and smoke derived from burning of C3 and C4 grasses. 41, 263-269.

Guo, Z., Jiang, W., Chen, S., Sun, D., Shi, L., Zeng, G., Rui, M.J.A.R., 2016. Stable isotopic compositions of elemental carbon in PM1. 1 in north suburb of Nanjing Region, China. 168, 105-111.

Huang, L., Brook, J., Zhang, W., Li, S., Graham, L., Ernst, D., Chivulescu, A., Lu, G., 2006. Stable isotope measurements of carbon fractions (OC/EC) in airborne particulate: A new dimension for source characterization and apportionment. Atmospheric Environment 40, 2690-2705.

Kawashima, H., Haneishi, Y., 2012. Effects of combustion emissions from the Eurasian continent in winter on seasonal δ 13 C of elemental carbon in aerosols in Japan. Atmospheric environment 46, 568-579.

Levin, I., Naegler, T., Kromer, B., Diehl, M., Francey, R.J., Gomez-Pelaez, A.J., Steele, L.P., Wagenbach, D., Weller, R., Worthy, D.E., 2010. Observations and modelling of the global distribution and long-term trend of atmospheric 14CO2. Tellus 62, 26-46.

Liu, G., Li, J., Xu, H., Wu, D., Liu, Y., Yang, H.J.A.e., 2014. Isotopic compositions of elemental carbon in smoke and ash derived from crop straw combustion. 92, 303-308.

López-Veneroni, D., 2009. The stable carbon isotope composition of PM 2.5 and PM 10 in Mexico City Metropolitan Area air. Atmospheric Environment 43, 4491-4502.

Mohn, J., Szidat, S., Fellner, J., Rechberger, H., Quartier, R., Buchmann, B., Emmenegger, L., 2008. Determination of biogenic and fossil CO2 emitted by waste incineration based on (CO2)-C-14 and mass balances. Bioresource Technology 99, 6471-6479.

Wang, G., Yao, J., Zeng, Y., Huang, Y., Qian, Y., Liu, W., Li, Y., Yuan, N., Liu, S., Shan, J., 2013. Source Apportionment of Carbonaceous Particulate Matter in a Shanghai Suburb Based on Carbon Isotope

214 Composition. Aerosol Science and Technology 47, 239-248.
215 Widory, D., 2006. Combustibles, fuels and their combustion products: A view through carbon isotopes.
216 Combustion Theory and Modelling 10, 831-841.
217 Zhu, S., Ding, P., Wang, N., Shen, C., Jia, G., Zhang, G., 2015. The compact AMS facility at Guangzhou
218 Institute of Geochemistry, Chinese Academy of Sciences. Nuclear Instruments & Methods in Physics
219 Research 361, 72-75.
220